Available online at www.sciencedirect.com
SCIENCE DIRECT®
International Journal of Heat and Mass Transfer 47 (2004) 5629–5638
International Journal of HEAT and MASS TRANSFER
www.elsevier.com/locate/ijhmt

Mathematical modeling of heat transfer, condensation, and capillary flow in porous insulation on a cold pipe

M.K. Choudhary [a,*], K.C. Karki [b], S.V. Patankar [b]

[a] Owens Corning Science & Technology, Granville, OH 43023, USA
[b] Innovative Research, Inc., Plymouth, MN 55447, USA

Received 31 December 2003; received in revised form 14 July 2004
Available online 16 September 2004

Abstract

Porous insulation used on pipes carrying cold fluids suffers thermal degradation due to condensation of water vapor and the build up of water in the insulation. Recently, it has been suggested that the thermal degradation can be significantly reduced by wrapping a hydrophilic wick fabric on the cold pipe. The capillary action of the fabric, aided by gravity, allows the condensed moisture to move to the outer surface of the insulation, from where, if ambient conditions are right, it evaporates. This paper presents the details of a mathematical model for condensation in the insulation in the presence of the wick fabric. The model is based on the volume-averaged equations for unsteady transport of heat, water vapor, and liquid water in a porous medium. The wick is modeled as an anisotropic porous medium. The model also allows for the presence of a vapor retarder jacket that is used to reduce the ingress of water vapor into the insulation. The model has been applied to an insulation layer around a horizontal pipe. The presence of the wick is shown to significantly reduce the amount of liquid water in the insulation. The results of the model have been verified using laboratory experiments and field tests.
© 2004 Elsevier Ltd. All rights reserved.

1. Introduction

Porous insulation used on pipes carrying cold fluids suffers thermal degradation due to condensation of water vapor and the build up of water in the insulation. A porous insulation, such as fiberglass insulation, typically consists of a solid matrix (i.e. glass fibers) and air–water vapor mixture. As the temperature within the insulation decreases, the moisture already present in the insulation may condense. In practice, the porous insulation is covered with a jacket, referred to as the "vapor retarder" which, as the name suggests, aims to reduce the ingress of water vapor into the insulation. However, depending upon the permeance (conductance for mass diffusion) of the vapor retarder jacket, there will always be a small amount of air infiltration into the insulation. Moreover cracks and flaws inevitably occur in the jacket, and as a result, much more air infiltration than that suggested by the permeance rating of the jacket takes place. The air brings with it water vapor whose amount depends upon the ambient humidity. The water vapor in the insulation condenses when the local vapor concentration exceeds the equilibrium concentration corresponding to the local temperature, that is, when the vapor temperature

* Corresponding author. Tel.: +1 740 321 7343; fax: +1 740 321 4343.
E-mail address: manoj.choudhary@owenscorning.com (M.K. Choudhary).

0017-9310/$ - see front matter © 2004 Elsevier Ltd. All rights reserved.
doi:10.1016/j.ijheatmasstransfer.2004.07.016

Nomenclature

A, B	constants in the expression for saturation vapor pressure, Eq. (8)
c_p	specific heat (J/kg K)
D	binary diffusion coefficient for transport of water vapor (m^2/s)
D_l	liquid diffusivity (kg/m s), Eq. (16)
$\mathbf{g}$	acceleration due to gravity (m/s^2)
h_c	heat transfer coefficient at the outer surface of insulation (W/m^2 K)
$h_{c,eff}$	effective heat transfer coefficient at the outer surface of insulation (W/m^2 K), Eq. (20)
h_{fg}	latent heat of vaporization (J/kg)
h_m	mass transfer coefficient at the outer surface of insulation (kg/m^2 s)
$h_{m,eff}$	effective mass transfer coefficient at the outer surface of insulation (kg/m^2 s), Eq. (21)
K	absolute permeability (m^2)
k_{eff}	effective thermal conductivity (W/m K), Eq. (13)
k_{rl}	relative permeability for liquid flow, Eq. (14)
M	molecular weight (kg/kmol)
$\dot{m}'''$	rate of phase change (negative for condensation) (kg/m^3 s)
p	pressure (Pa)
p_c	capillary pressure (Pa)
R	universal gas constant (=8314 J/kmol K)
S	dimensionless liquid saturation, Eq. (15)
s	phase saturation
s_l^0	critical liquid saturation, Eq. (15)
T	temperature (deg C)
t	time (s)
y_v	mass fraction of water vapor in the gaseous mixture

Greek symbols

ε	porosity
μ	dynamic viscosity (kg/m s)
v	kinematic viscosity (m^2/s)
ρ	density (kg/m^3)
σ	coefficient of surface tension (N/m)
ζ	hindrance function, Eq. (18)
$\langle \rho c_p \rangle$	effective heat capacity of insulation matrix, Eq. (12)

Subscripts

g	gas
l	liquid
s	solid
v	vapor
a	air
sat	saturation condition

becomes equal to its local saturation value. Condensation is accompanied with the release of the latent heat of vaporization, which acts as a heat source in the heat transport process. The accumulation of water results in an increase in effective thermal conductivity of the insulation and a decrease in the effective vapor diffusion coefficient. Both these factors affect heat transfer and condensation rate in the insulation. Thus, a basic understanding of simultaneous heat and mass transfer in the presence of condensation in porous insulation is important in the design of effective insulation systems.

Because of its practical importance, the problem of thermal degradation of porous insulation due to moisture condensation has been studied, using mathematical models as well as experimental methods, by several investigators. The experimental studies [1–6] have been limited to simple geometries, such as slabs, and have focused on the basic heat and mass transfer processes in the insulation layer. The modeling studies cover the full gamut from analytical approaches [7–11] valid for constant properties and other simplifying assumptions such as "quasi steady state" behavior to numerical solution of the governing heat and mass transport equations [12–15]. These earlier studies provide valuable insights into the impact of condensation on the thermal degradation of insulation applied on cold surfaces.

In order to retain the thermal effectiveness of porous insulation applied on cold pipes, Korsgaard [16] has patented a concept that involves wrapping the surface of the cold pipe with a hydrophilic (i.e., having an affinity for water) wick fabric and enclosing the pipe-wick assembly inside the insulation. The capillary action of the fabric, in combination with gravity, allows the condensed moisture to move to the outer surface of the insulation, from where, if ambient conditions are right, it evaporates. This process of removal of condensed moisture provides a means for keeping the insulation dry and its thermal characteristics relatively intact. Products based on this concept are already in commercial use (e.g., Vapor-Wick® from Owens Corning).

In the present work, we develop and illustrate a transient, two-dimensional mathematical model for simultaneous heat and mass transfer in porous insulation on cold pipes. The model presented here is based on the volume-averaged equations for unsteady transport of heat, water vapor, and liquid water in a porous medium. A significant, novel feature of this model is that it incorporates transport processes in a hydrophilic wick fabric

wrapped around the cold pipe and extending through the insulation. The wick fabric is modeled as a porous medium with anisotropic flow permeability. The model includes the effect of liquid water on physical properties such as the thermal conductivity and vapor diffusivity.

2. Mathematical model

2.1. Physical situation

The physical situation for which we seek to develop a mathematical model is shown in Fig. 1. The system consists of the following components:

(a) A pipe carrying a cold fluid at temperature T_c.
(b) A hydrophilic wick fabric wrapped around the pipe.
(c) The insulation matrix.
(d) A vapor retarder to retard the ingress of water vapor into the insulation.

The ambient air is at the temperature T_a and relative humidity RH. Since the ambient temperature T_a is greater than the cold pipe surface temperature T_c, there will be heat flux from the outside into the insulation. Furthermore, the vapor pressure of water vapor increases exponentially with temperature. Thus, under humid conditions there is a potential for water vapor diffusion from the ambient into the insulation. This water vapor will condense in the insulation matrix and at the wick surface in contact with the cold pipe (condensation can potentially occur wherever the vapor temperature is equal or less than the saturation temperature). The presence of a hydrophilic wick fabric provides a means for removing the condensed moisture out of the insulation matrix. With the downward orientation of the wick, as shown in Fig. 1, both capillary and gravity participate in the water removal process. The water is transported to the outer surface of the vapor-retarding jacket and allowed to evaporate from the wick surface. In practice, the protruding part of the wick fabric is wrapped around the vapor retarder. However, in the model to be described here, we will assume that the wick terminates at the end of the insulation.

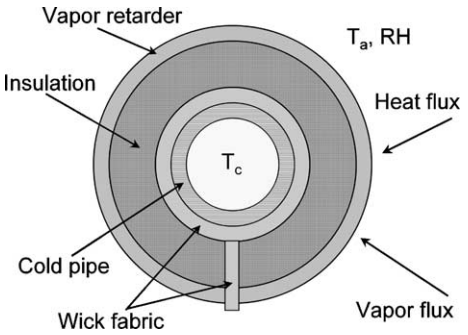

Fig. 1. Description of physical phenomena involved in the Vapor wick concept. T_c is the cold-pipe temperature, T_a is the ambient temperature, and RH is the relative humidity.

2.2. Governing equations

Three phases are present in a wet insulation: (i) the solid matrix, (ii) the liquid water, and (iii) the gaseous phase composed of air and water vapor. The governing equations for a porous medium are obtained by applying the local volume averaging technique [17] to the mass, momentum, and energy equations for individual phases.

The computational model is constructed for the horizontal orientation of the pipe and transport processes are assumed to be two-dimensional (r,θ). This simplification allows the construction of an efficient computational model while preserving the essential features of the physical phenomena taking place in the system considered here. Further, since the geometry, initial conditions, and boundary conditions are symmetric about the vertical direction, computations were made only for one-half of the cross section. The other simplifying assumptions are listed below.

(a) Convection in the insulation matrix is neglected.
(b) The insulation matrix is homogeneous.
(c) The total gas-phase pressure in the insulation matrix is constant.
(d) The solid–liquid–gas system is in local thermal equilibrium.
(e) Dry air is stagnant in the insulation matrix. However, water vapor is mobile.

Similar assumptions have been made, among others, by Vafai and Whitaker [12] and Wijeysundera et al. [15]. The final volume-averaged equations are stated below.

Gas-phase diffusion equation (diffusion of water vapor)

$$\frac{\partial}{\partial t}(\varepsilon\rho_g s_g y_v) = \nabla\cdot(\varepsilon\rho_g s_g D\nabla y_v) + \dot{m}'''. \tag{1}$$

Energy equation

$$\langle\rho c_p\rangle\frac{\partial T}{\partial t} = \nabla\cdot(k_{eff}\nabla T) - \dot{m}'''h_{fg}. \tag{2}$$

Liquid transport equation

$$\frac{\partial}{\partial t}(\varepsilon\rho s_l) = \nabla\cdot(D_l\nabla s_l) - \nabla\cdot\left(\zeta K\frac{k_{rl}}{\nu_l}\rho_l g\right) - \dot{m}'''. \tag{3}$$

Here the symbols s_g and s_l denote the phase saturation for gas and liquid phase, respectively. The phase saturation for a specific phase is defined as the volumetric

fraction of the void space occupied by the phase. Other symbols are defined in the Nomenclature.

2.3. Supplementary relationships

The governing transport equations need to be supplemented by the following relationships.

2.3.1. Volumetric constraint

$$s_l + s_g = 1. \tag{4}$$

2.3.2. Thermodynamic relations

Vapor pressure

$$p_v = \rho_v \left[\frac{R}{M_v}\right] T. \tag{5}$$

Air pressure

$$p_a = \rho_a \left[\frac{R}{M_a}\right] T. \tag{6}$$

Total gas pressure

$$p_{total} = p_v + p_a. \tag{7}$$

Saturation water vapor pressure

$$p_{v,sat} = A \exp\left[-B\left(\frac{1}{T} - \frac{1}{T_0}\right)\right]. \tag{8}$$

The constants are: $A = 3567$ Pa, $B = 5232$ K, and $T_0 = 300$ K.

Saturation water vapor mass fraction

$$y_{v,sat} = \frac{M_v p_{v,sat}}{M_v p_{v,sat} + M_a (p_{total} - p_{v,sat})}. \tag{9}$$

2.4. Thermodynamic and transport properties

Density of water vapor–air mixture

$$\rho_g = \rho_v + \rho_a. \tag{10}$$

Specific heat of water vapor–air mixture

$$c_{pg} = y_v c_{pv} + (1 - y_v) c_{pa}. \tag{11}$$

Effective heat capacity of insulation matrix

$$\langle \rho c_p \rangle = (1 - \varepsilon)\rho_s c_{ps} + \varepsilon[s_g \rho_g c_{pg} + s_l \rho_l c_{pl}]. \tag{12}$$

Effective thermal conductivity

$$k_{eff} = (1 - \varepsilon)k_s + \varepsilon(s_l k_l + s_g k_g). \tag{13}$$

Relative permeability for liquid [18]

$$k_{rl} = S^n. \tag{14}$$

The exponent n is taken as 3. The dimensionless liquid saturation S is defined as

$$S = \frac{s_l - s_l^0}{1 - s_l^0}. \tag{15}$$

The critical liquid saturation s_l^0 is taken as 0.09 for insulation and 0.8 for wick fabric.

Liquid diffusion coefficient (due to capillary forces)

$$D_l = -K \frac{k_{rl}}{v_l} \frac{dp_c}{ds_l}. \tag{16}$$

Capillary pressure [18]

$$p_c = \sigma\left(\frac{\varepsilon}{K}\right)^{1/2} [1.417(1 - S) - 2.120(1 - S)^2 + 1.263(1 - S)^3]. \tag{17}$$

Hindrance function

$$\zeta = \frac{(v_l/v_g)(1 - S)^n}{S^n + (v_l/v_g)(1 - S)^n}. \tag{18}$$

The hindrance function varies from 0 to 1. It has a value of 1 in regions that contain no liquid and 0 in regions that are fully saturated with liquid.

The thermal conductivity of moist insulation depends on the distribution of liquid within the insulation. Alternative formulas for effective conductivity assume different liquid distributions. The present formula, Eq. (13), assumes that the liquid is distributed in continuous layers parallel to the direction of heat flow. Among various formulas, it is expected to produce largest heat and moisture gains.

2.5. Representation of the wick

The present model incorporates a simplified representation of the wick. The wick fabric, which is wrapped around the cold pipe and protrudes through part of the outer boundary, is modeled as a porous medium with anisotropic permeability. The permeability along the length of the wick is assigned a higher value than that across the thickness. In addition, the critical liquid saturation – the liquid saturation level that must be exceeded for the liquid to become mobile – is taken as 0.8. This high value for the critical liquid saturation allows the wick to become very nearly saturated before the wicking action begins.

2.6. Initial and boundary conditions

2.6.1. Initial conditions

Initially, the insulation matrix is taken as completely dry and water vapor concentration is taken as zero. The steady-state temperature distribution in an annulus with specified temperatures at the inner and outer surfaces is specified as the initial temperature distribution in the insulation:

$$T(r) = \frac{T_{in} - T_{out}}{\ln(r_{in}/r_{out})} \ln\left(\frac{r}{r_{out}}\right) + T_{out}. \quad (19)$$

Here the subscripts "in" and "out" refer to the inner and outer surfaces of the annulus.

2.6.2. Boundary conditions

At time $t = 0$, the outer surface is exposed to humid ambient conditions. The treatment of boundary conditions is as follows:

At the *inner surface* ($r = r_{in}$), the temperature is specified (T_{in}). For water vapor and liquid transport, this boundary is treated as impermeable, i.e., the diffusion flux is zero.

At the *symmetry boundary* ($\theta = 0$ and π), gradient normal to the surface is set equal to zero for all variables.

The *outer surface* ($r = r_{out}$) is exposed to the environment with known temperature and relative humidity (water vapor mass fraction). For temperature and water vapor equations, heat and mass transfer coefficients are specified. The heat transfer coefficient is calculated for free convection between the surface and the surrounding fluid. The mass transfer coefficient is deduced from the analogy between heat and mass transfer. When a vapor retarder is present at the outer surface, these coefficients include the additional resistance due to the retarder. (The representation of vapor retarder in the model is treated in greater detail in the following section.) For liquid transport, this boundary is modeled as impermeable. In the presence of a wick, that portion of the outer surface through which the wick protrudes is regarded as a "flaw" in the vapor retarder, and the resistance of the vapor retarder is ignored over this region. For liquid transport, the condition of free drainage (zero gradient of liquid saturation) is imposed over the wick portion of the outer surface. This condition allows the liquid water to flow out of the wick by gravity.

2.6.3. Representation of vapor retarder

A vapor retarder is a thin plastic sheet (thickness $\sim 1.0 \times 10^{-4}$ m) that is wrapped on the outer surface of the insulation layer to reduce diffusion of water vapor from the surrounding environment to the insulation. Due to its very small thickness, the physical extent of the retarder is not represented in the model. Instead, as noted above, its effect is included in the heat and mass transfer coefficients at the outer surface. Thus the outer boundary of the computational domain coincides with the inner surface of the vapor retarder.

The effective heat and mass transfer coefficients at the outer surface are calculated as

$$\frac{1}{h_{c,eff}} = \frac{1}{h_c} + \frac{\delta_{ret}}{k_{ret}}, \quad (20)$$

$$\frac{1}{h_{m,eff}} = \frac{1}{h_m} + R_{ret}. \quad (21)$$

In these equations, δ_{ret} is the thickness of the vapor retarder, k_{ret} is the thermal conductivity of the retarder material, R_{ret} is the resistance of the retarder to water vapor diffusion, and h_c and h_m are the heat and mass transfer coefficients at the outer surface. The value of R_{ret} is calculated from the permeance (specified in perms) of the vapor retarder as follows:

$$R_{ret} = \frac{M_v}{M_m p_{total}(\text{permeance} \times 5.7 \times 10^{-11})}. \quad (22)$$

In Eq. (22), M_v and M_m are the molecular weights of water vapor and the air–water vapor mixture, respectively, and p_{total} is the total gas pressure in the system.

3. Numerical solution procedure

The mathematical model presented above was implemented as an adaptation of the COMPACT computational fluid dynamics (CFD) program [19]. COMPACT program uses the finite-volume formulation to discretize the conservation equations. The fully implicit scheme is used for discretization of the unsteady terms, and central differencing is used for the diffusion terms. The discrete equations are solved using the line-by-line tri diagonal matrix algorithm (TDMA) supplemented by the block-correction technique. Complete details of the numerical method are available in [20].

The solution of the governing equations proceeds as follows:

1. Assume $\dot{m}'''$ is zero everywhere. That is, there is no phase change.
2. Solve the equations for water vapor mass fraction, Eq. (1), and for temperature, Eq. (2).
3. Compare the calculated water vapor concentration with the equilibrium (saturation) concentration corresponding to the saturation vapor pressure at the local temperature. Note that the saturation vapor pressure is given by Eq. (8) and the corresponding mass fraction by Eq. (9).
   (a) If the calculated water vapor concentration is larger than the equilibrium value, set the local concentration equal to the equilibrium value. At these points, use Eq. (1) to calculate the rate of condensation.
   (b) If the calculated concentration is less than the local equilibrium value, no special measures are taken.
4. Solve the equation for liquid saturation, Eq. (3).
5. Return to Step 2 and repeat until convergence.

4. Computed results and discussion

In this section, we will discuss computed results for the following two cases:

- *Case 1:* No wick applied on the cold pipe (i.e., fiberglass insulation is applied directly on the cold pipe).
- *Case 2:* A wick fabric is wrapped around the cold pipe before applying the insulation.

In both cases, the vapor retarder has a permeance of 1 perm ($=5.7\times10^{-11}$ kg/m^2 s Pa) and the ambient conditions are 305.5 K, 90% relative humidity. The geometric parameters and the operating conditions used in the computations are summarized in Table 1. The physical property values are summarized in Table 2. It should be noted that the values used in Tables 1 and 2 have been selected to illustrate the modeling approach and do not refer to any actual pipe insulation system in use.

Results presented here were obtained on a non-uniform computational mesh comprising 32 control volumes in the radial direction and 24 control volumes in the angular direction. The grid spacing was finer near the inner surface and within the wick region. A variable time-step size, varying from 30 to 7200 s, was used; smaller time steps were used at the beginning and when the liquid water began to move. The chosen computational grid and the time-step size were decided by making a number of initial exploratory runs. The results of these runs indicate that the reported results are accurate to within 2%.

Table 1
Geometric parameters and operating conditions

Parameter	Value
Outer radius of cold pipe	0.0167 m
Thickness of insulation layer	0.0254 m
Thickness of wick fabric	3.2×10^{-4} m
Thickness of vapor retarder	1×10^{-4} m
Porosity of insulation layer	0.9756
Porosity of wick fabric	0.86
System pressure	1.013×10^{5} Pa
Ambient temperature	305 K
Ambient relative humidity	90%
Cold pipe temperature	275 K
Heat transfer coefficient	7 W/m^2 K
Mass transfer coefficient	7.5×10^{-3} kg/m^2 s

The present model was also used to predict the diffusion and condensation of water vapor in fiberglass slab insulation and the results were compared with those given by the analytical model of Wijeysundera et al. [10]. The values of heat and vapor fluxes at the outer surface and the locations of the dry–wet boundaries, for a wide range of operating conditions, agreed to within 5%.

Fig. 2 shows liquid saturation level and temperature distribution in insulation after 250 days of operation for Case 1 (i.e., without the wick). As seen in this figure, the region in the vicinity of the cold pipe is essentially completely saturated with condensed water. This zone of saturation would keep on expanding with time till the whole cross section of insulation becomes saturated.

Table 2
Physical property values used in computation

Property	Value
Surface tension	0.078 N/m
Latent heat of vaporization	2.501×10^{6} J/kg
Specific heat of solid matrix	880 J/(kg K)
Specific heat of liquid water	4200 J/(kg K)
Specific heat of air	1005 J/(kg K)
Specific heat of water vapor	1820 J/(kg K)
Thermal conductivity of air–water vapor mixture	0.027 W/(m K)
Thermal conductivity of solid matrix	0.15 W/(m K)
Thermal conductivity of liquid water	0.63 W/(m K)
Dynamic viscosity of liquid water	1×10^{-3} kg/m s
Dynamic viscosity of air	2×10^{-5} kg/m s
Density of solid matrix	2500 kg/m^3
Density of liquid water	1000 kg/m^3
Diffusivity of water vapor in air	2.5×10^{-5} m^2/s
Permeability of insulation layer	5.0×10^{-10} m^2
Permeability of wick fabric (This is the permeability along the longitudinal direction. The permeability along the transverse direction (i.e., along the thickness) is taken as one-tenth of this value.)	1.0×10^{-10} m^2
Permeance of vapor retarder	1 perm (5.7×10^{-11} kg/(m^2 s Pa))
Thermal conductivity of vapor retarder	0.05 W/m K

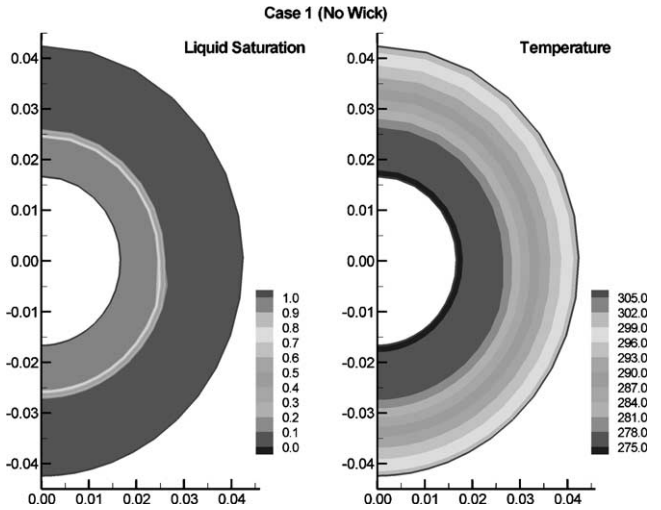

Fig. 2. Condensed moisture (saturation level) and temperature distribution for Case 1 (without wick) after 250 days of operation. Temperature values are in K.

Similarly, the condensation front will continuously move toward the outer surface of the insulation.

Fig. 3 shows the amount of water gained by insulation (over 1 m length of pipe) and the effective thermal conductivity ratio (effective conductivity normalized by its dry insulation value) as functions of time. (The effective conductivity is defined as the conductivity of dry insulation layer that will give a steady-state heat flux equal to the local heat flux under the same temperature conditions.) As seen in Fig. 3, in 500 days of operation, the insulation picks up about 2.5 kg of water. It should be recalled that the calculations are for the case where the ambient conditions remain constant at 305 K and 90% relative humidity and the vapor retarder has a permeance of 1 perm. Because the thermal conductivity of liquid water is much higher (about 17 times) than that of dry insulation, with the gain in water the conductivity of the insulation layer increases (i.e., its insulation value decreases) and, in 500 days of operation, the effective thermal conductivity ratio approaches a value of 3.

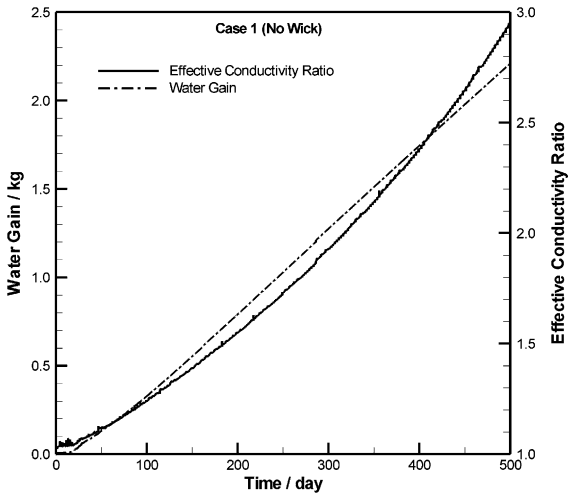

Fig. 3. Water gain (in kg) and the effective thermal conductivity ratio with time for Case 1.

In the next series of figures, let us examine the impact of using a wick around the cold pipe. Fig. 4 shows the distributions of liquid saturation and temperature for Case 2 after 15 days of operation. In about 15 days, the wick allows the system to reach a state of equilibrium whereby the amount of moisture condensing in the insulation equals the amount being drained through the wick. We can see that the wick keeps most of the insulation dry, and it is only near the bottom and in the vicinity of the wick fabric that the insulation retains some moisture. (It should be noted that the glass fiber insulation is hydrophobic because of organic binders used in the manufacture of insulation. This property is not accounted for in the model described here. In practice, the insulation with a wick fabric has been found to be dry with water present only in the wick.) As for the temperature distribution, the condensation front is confined to a small region close to the wick.

Fig. 5 compares the amount of water gained and the effective thermal conductivity ratio for the two cases. The results for Case 1 are the same as those shown earlier in Fig. 3. Note that the X-axis scale in Fig. 5 changes after $t = 50$ days. As seen here, with the use of wick, the system achieves a state of equilibrium in about 15 days and after that, as long as the ambient conditions remain unchanged, the insulation does not gain any more water. It is also seen that the amount of water gained in Case 2

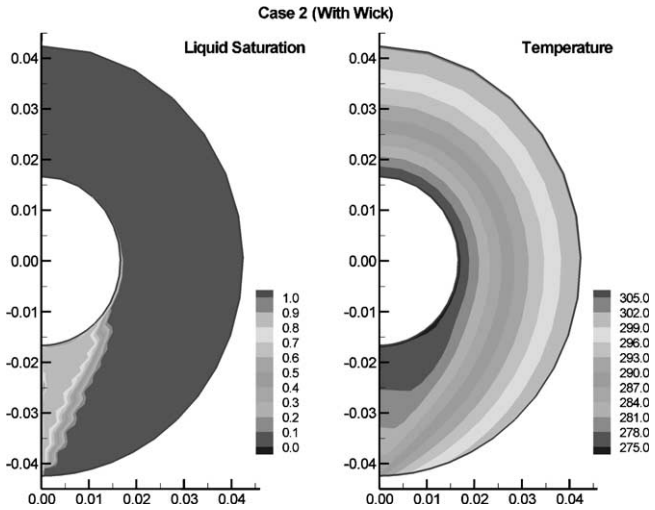

Fig. 4. Condensed moisture (saturation level) and temperature distribution for Case 2 (with wick) after 15 days of operation. Temperature values are in K.

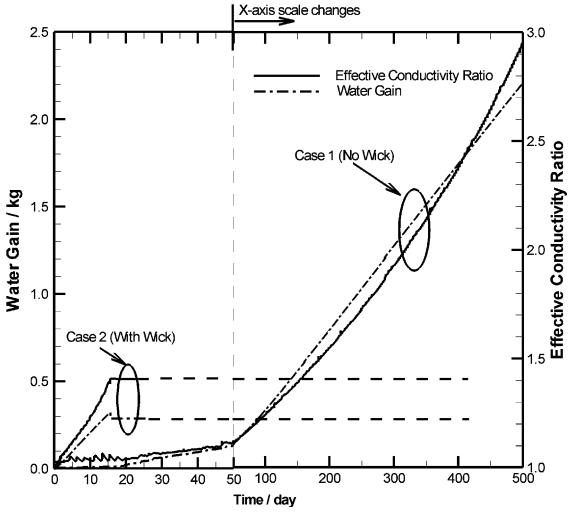

Fig. 5. Water gain (in kg) and the effective thermal conductivity ratio with time for Case 1 (without wick) and Case 2 (with wick). Please note that the *X*-axis scale changes after 50 days.

is much smaller than that in that in Case 1. However, the initial *rate of gain of water* in Case 2 is actually higher than that in Case 1. In other words, until the wicking action commences, the presence of wick actually enhances the diffusion of water vapor into the system. This is because the wick section on the outer boundary is not covered by the vapor retarder; this section, therefore, offers relatively low resistance for the vapor flow and facilitates the transport of humid air into the insulation. The water vapor begins to condense as it approaches the cold region near the inner surface of the pipe. Once the condensation begins, the presence of liquid water propagates cold temperatures away from the inner surface. Due to the anisotropic nature of the wick fabric, the movement of liquid water is confined to the wick section. The initial transport of water vapor and its subsequent condensation help in establishing nearly saturated conditions within the wick and hence in initiating the wicking action. The transport of water vapor diminishes once water begins to condense in the wick fabric.

The wick, by limiting the amount of water in the insulation, also limits the increase in the effective conductivity. The effective thermal conductivity ratio for Case 2 reaches a steady-state value of about 1.4. For Case 1, however, the effective thermal conductivity ratio keeps on increasing with time (i.e., the insulation performance continues to deteriorate), and in 500 days of operation, reaches a value of about 3. The wick, therefore, provides a means to significantly limit the deterioration in insulation performance due to the presence of water.

The mathematical modeling study described in this paper was complemented by laboratory experiments and field trials of the VaporWick® product. Fig. 6 shows experimental results on water gain by three VaporWick® pipe sections placed in a humidity chamber under the conditions of 306 K and 80% relative humidity. The pipe sections were 0.91 m long, the outside diameter of the cold pipe was 0.029 m, and the insulation thickness was 0.036 m. The cold surface temperature was 275 K. The vapor retarder had the permeance of 0.15 perm. The three pipe sections used three different wicking fabrics. The conditions used in the experiments were quite different from those used in the mathematical modeling calculations described earlier. However, the experimental findings are qualitatively similar to the modeling

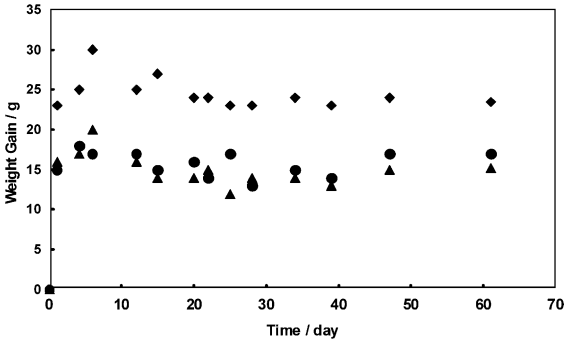

Fig. 6. Weight gain of three Vaporwick® pipe sections placed in a humidity chamber at 306 K and 80% relative humidity.

results. Initially, there is a relatively rapid gain of water. This is followed by the onset of the wicking action and drop in the amount of water, culminating in a plateau in the weight gain vs. time curve. Subsequent disassembly and examination of the specimens revealed that liquid moisture was confined to the wick material while the insulation remained dry.

The VaporWick® product has been installed in several locations with oldest application being more than 3 years old. A follow-up study of the oldest application at the end of the three-year period found the insulation to be dry. Thus both laboratory and field studies appear to confirm the modeling finding that a properly designed pipe insulation system incorporating the wicking concept is effective in getting the condensed moisture out of the insulation.

5. Concluding remarks

A comprehensive mathematical formulation was developed to describe water vapor diffusion, liquid water flow, and heat transfer in a porous insulation applied on pipes carrying cold fluids. The principal advance made in this work is in coupling transport phenomena in the insulation with those in wick fabric wrapped around the pipe. The model also incorporates a vapor retarder jacket that is used to reduce the ingress of water vapor into the insulation. The use of the wick fabric allows the condensed liquid water to be taken out of the insulation by the combined action of gravity and capillary. The governing transport equations together with the initial and the boundary conditions and the supplementary relationships were solved numerically to investigate the thermal performance of two insulation systems, one without the wick and the other with the wick. Calculated results for temperature and water concentration showed the use of a wick could be effective in removing water from the insulation and maintaining its insulation value. Laboratory experiments and field trials conducted to-date appear to confirm the modeling finding that a properly designed pipe insulation system incorporating the wicking concept is effective in getting the condensed moisture out of the insulation.

In a broader sense, the paper has provided a general model to investigate transient flow, heat transfer, and phase change phenomena in porous materials.

Acknowledgments

The authors are grateful to Ms. Roberta Alkire for her encouragement and support of this work and to members of the VaporWick® Team, especially Mr. Roy Shaffer for providing insights into the wetting characteristics of various fabrics. The authors gratefully acknowledge the use of experimental results obtained by Mr. Shaffer, Dr. Patrick Aubourg, and Dr. Qingyu Zeng. The authors also thank Ms. Alkire, Mr. Neil Hettler, Mr. Patrick Dean, Mr. David Cox, Mr. Steve Barns, and Mr. Frank O'Brien-Bernini for allowing the publication of this paper.

References

[1] M.K. Kumaran, Moisture transport through glass-fibre insulation in the presence of a thermal gradient, Journal of Thermal Insulation 10 (1987) 243–255.
[2] M.K. Kumaran, Comparison of simultaneous heat and moisture transport through glass-fibre and spray-cellulose insulations, Journal of Thermal Insulation 12 (1988) 6–16.
[3] C. Langlais, M. Hyrien, S. Klarsfeld, Influence of moisture on heat transfer through fibrous insulating materials, in: F.A. Govan, D.M. Greason, J.D. McAllister (Eds.), ASTM Special Technical Publication 789, 1981, pp. 563–581.
[4] C. Langlais, S. Klarsfeld, Heat and mass transfer in fibrous insulations, Journal of Thermal Insulation 8 (1984) 49–80.
[5] W.C. Thomas, G. Bal, R.J. Onega, Heat and moisture transfer in a glass fiber roof-insulating material, in: F.A. Govan, D.M. Greason, J.D. McAllister (Eds.), ASTM Special Technical Publication 789, 1981, pp. 582–601.
[6] C.P. Hedlin, Heat transfer in a wet porous thermal insulation in a flat roof, Journal of Thermal Insulation 11 (1988) 165–188.
[7] S. Motakef, M.A. El-Masri, Simultaneous heat and mass transfer with phase change in a porous slab, International Journal of Heat and Mass Transfer 29 (1986) 1503–1512.
[8] A.P. Shapiro, S. Motakef, Unsteady heat and mass transfer with phase change in porous slabs: analytical solutions and experimental results, International Journal of Heat and Mass Transfer 33 (1990) 163–173.
[9] N.E. Wijeysundera, B.F. Zheng, M. Iqbal, E.G. Hauptmann, Effective thermal conductivity of flat-slab and round-pipe insulations in the presence of condensation, Journal of Thermal Insulation and Building Envelopes 17 (1993) 55–77.

[10] N.E. Wijeysundera, M.N.A. Hawaldar, Y.T. Tan, Water vapour diffusion and condensation in fibrous insulations, International Journal of Heat and Mass Transfer 32 (1989) 1865–1878.
[11] W.J. Chang, C.I. Weng, An analytical solution to coupled heat and moisture diffusion in porous materials, International Journal of Heat and Mass Transfer 43 (2000) 3621–3632.
[12] K. Vafai, S. Whitaker, Simultaneous heat and mass transfer accompanied by phase change in porous insulation, ASME Journal of Heat Transfer 108 (1986) 132–140.
[13] K. Vafai, H.C. Tien, A numerical investigation of phase change effects in porous materials, International Journal of Heat and Mass Transfer 32 (1989) 1261–1277.
[14] Y.X. Tao, R.W. Besant, K.S. Rezkallah, The transient thermal response of a glass-fiber insulation slab with hygroscopic effects, International Journal of Heat and Mass Transfer 35 (1992) 1155–1167.
[15] N.E. Wijeysundera, B.F. Zheng, M. Iqbal, E.G. Hauptmann, Numerical simulation of the transient moisture transfer through porous insulation, International Journal of Heat and Mass Transfer 39 (1996) 995–1004.
[16] V. Korsgarrd, Insulation system for conduit or container wherein inner and outer water-absorbing layers connect through slot in intermediate heat-insulating layer, US Patent No. 5441083 (1995).
[17] S. Whitaker, Simultaneous heat, mass and momentum transfer in porous media: a theory of drying, Advances in Heat Transfer 13 (1977) 119–203.
[18] M. Kaviany, Principles of Heat Transfer in Porous Media, Springer, Berlin, 1991.
[19] Innovative Research, Inc., Reference Manual for COMPACT-2D, Innovative Research, Inc., Minneapolis, MN, USA, 2001.
[20] S.V. Patankar, Numerical Heat Transfer and Fluid Flow, Hemisphere, New York, 1980.